PROCEEDINGS OF SPIE

SPIEDigitalLibrary.org/conference-proceedings-of-spie

Overview of Primitive Object Volatile Explorer (PrOVE) CubeSat or Smallsat concept

Pamela Clark, Tilak Hewagama, Shahid Aslam, James Bauer, Michael Daly, et al.

Pamela Clark, Tilak Hewagama, Shahid Aslam, James Bauer, Michael Daly, Lori Feaga, Dave Folta, Nicolas Gorius, Kyle Hughes, Terry Hurford, Donald Jennings, Timothy Livengood, Michael Mumma, Conor Nixon, Jessica Sunshine, Geronimo Villanueva, Kevin Brown, Ben Malphrus, Aaron Zucherman, "Overview of Primitive Object Volatile Explorer (PrOVE) CubeSat or Smallsat concept," Proc. SPIE 10769, CubeSats and NanoSats for Remote Sensing II, 107690J (18 September 2018); doi: 10.1117/12.2321264

SPIE.

Event: SPIE Optical Engineering + Applications, 2018, San Diego, California, United States

Overview of Primitive Object Volatile Explorer (PrOVE) Smallsat Concept

Pamela Clark*[1], Tilak Hewagama*[2,3], Shahid Aslam[3], James Bauer[2], Michael Daly[4], Lori Feaga[2], Dave Folta[3], Nicolas Gorius[5], Kyle Hughes[3], Terry Hurford[3], Donald Jennings[3], Tim Livengood[2,3], Michael Mumma[3], Conor Nixon[3], Jessica Sunshine[2], Geronimo Villanueva[3], Kevin Brown[6], Ben Malphrus[6], Aaron Zucherman[6]

1. Jet Propulsion Laboratory, California Institute of Technology, Pasadena, CA, 2. University of Maryland, College Park, MD, 3. NASA/GSFC, Greenbelt, MD, 4. York University, Toronto, CA 5. Catholic University of America, Washington DC, 6. Morehead State University, Morehead, KY

*Pamela.E.Clark@jpl.nasa.gov; phone 1 818 393-3262; fax 1 818 354-8887; jpl.nasa.gov

ABSTRACT

Here we describe the Primitive Object Volatile Explorer (PrOVE), a smallsat mission concept to study the surface structure and volatile inventory of comets in their perihelion passage phase when volatile activity is near peak. CubeSat infrastructure imposes limits on propulsion systems, which are compounded by sensitivity to the spacecraft disposal state from the launch platform and potential launch delays. We propose circumventing launch platform complications by using waypoints in space to park a deep space SmallSat or CubeSat while awaiting the opportunity to enter a trajectory to flyby a suitable target. In our Planetary Science Deep Space SmallSat Studies (PSDS3) project, we investigated scientific goals, waypoint options, potential concept of operations (ConOps) for periodic and new comets, spacecraft bus infrastructure requirements, launch platforms, and mission operations and phases. Our payload would include two low-risk instruments: a visible image (VisCAM) for 5-10 m resolution surface maps; and a highly versatile multispectral Comet CAMera (ComCAM) will measure 1) H2O, CO2, CO, and organics non-thermal fluorescence signatures in the 2-5 μm MWIR, and 2) 7-10 and 8-14 μm thermal (LWIR) emission. This payload would return unique data not obtainable from ground-based telescopes and complement data from Earth-orbiting observatories. Thus, the PrOVE mission would (1) acquire visible surface maps, (2) investigate chemical heterogeneity of a comet nucleus by quantifying volatile species abundance and changes with solar insolation, (3) map the spatial distribution of volatiles and determine any variations, and (4) determine the frequency and distribution of outbursts.

Keywords: cubesat, smallsat, comet, Oort Cloud, volatiles, flyby, Lagrange points

1. COMETS SIGNIFICANCE

Comets (**Figure 1**), which put on spectacular visual displays near perihelion, have long captured human imagination. Their glorious tails result from the intense solar radiation near ~1 AU that volatilizes material in the comet's nucleus. Over eons of inner Solar System (SS) perihelion passages, periodic comets suffer repeated exposures that permanently alter the states of their nuclei. By comparison, Oort cloud comets (OCCs) are new comets (**Figure 1**), making their first passage into the inner SS. OCCs are therefore nearly pristine and offer a direct window into the composition of the early SS. OCCs contain dust, organics, and ices – the same mix that potentially contributed the ingredients for life on Earth. Comets, for all their beauty, can also pose potential hazards to current-day life on Earth. PrOVE would provide additional understanding of the elusive members of this celestial class, helping to improve predictions about potential effects on modern Earth.

Primitive bodies, such as comets, are key to understanding SS formation (**Figure 2**). The structure and composition of cometary nuclei from comet reservoirs provide the best available guide to the condensation and evolution of matter within the early SS [1]. The relative abundance of volatile ices reflects the thermal and radiation history of cometary nuclei, leading a central role within cometary science. In the "Nice model," the current paradigm for dynamical sculpting of the early SS [2,3], comets that formed beyond ~17 AU from the proto-Sun, in the outer disk, were scattered into the Oort

CubeSats and NanoSats for Remote Sensing II, edited by Thomas S. Pagano, Charles D. Norton, Proc. of SPIE Vol. 10769, 107690J · © 2018 SPIE
CCC code: 0277-786X/18/$18 · doi: 10.1117/12.2321264

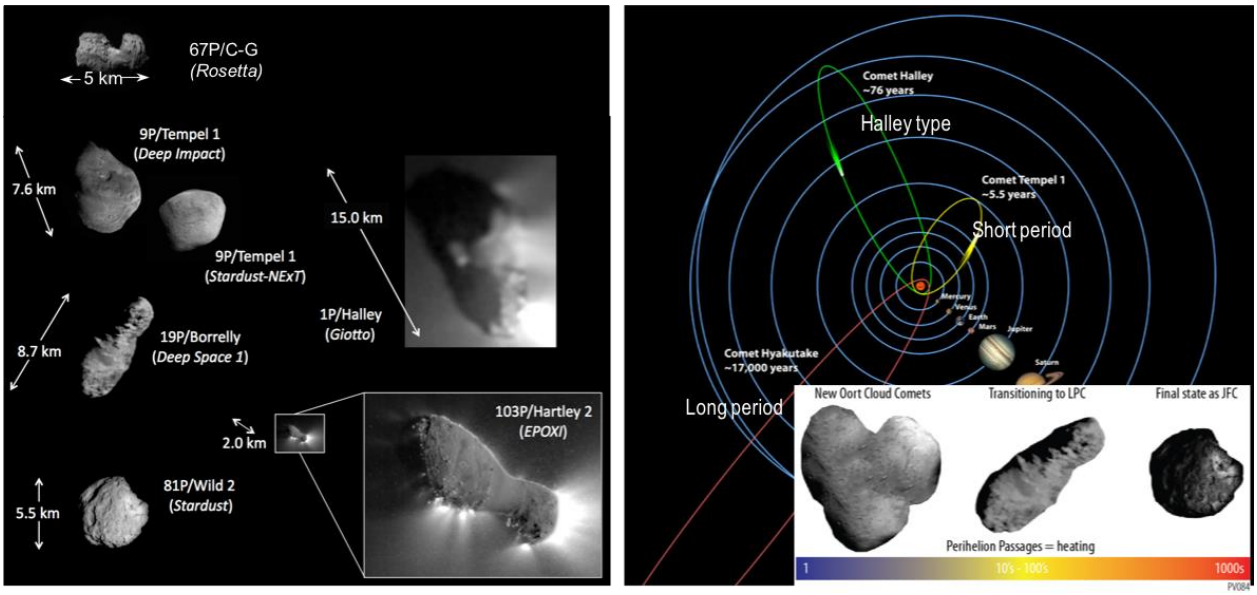

Figure 1: Comet images and origins. Left: Images of all cometary nuclei taken to date. Right: Typical orbits for three orbital classes of comets as discussed in the text: short period, Halley type, and long period. Oort cloud comets are long period. Insert Right: Oort cloud comet evolution as approaching perihelion.

cloud and Kuiper Belt reservoirs [4,5]. Comets that formed in the giant-planets region (5–14 AU) were ejected as the planets grew and also entered the Oort cloud and the higher-eccentricity Kuiper disk [6].
The dynamical mixing of the early SS is consistent with the significant chemical diversity found among even the modest number of studied comets [e.g., 1,7,8,9,10,11,12]. The chemical composition and dynamical classification of observed comets are not correlated, which is consistent with the blurring of the formation regions for Oort cloud and Kuiper Belt comets. Even if a large fraction of primitive objects in the Oort cloud were captured from the reservoirs of other stars in the Sun's birth cluster, it would present similar compositional diversity [13].

Most theories for the diversity of comets are relatively new, and the understanding of conditions in the early SS is far from complete. The Japan Aerospace Exploration Agency's (JAXA) Akari satellite surveyed 18 comets [14] and Deep Impact observed three comets [15,16,17], measuring CO_2 and CO abundance relative to H_2O with results that in some ways contradict current dynamical models [18]. In particular, the role of distance from the young Sun in setting the "snow line" at which various molecules condense is less clear. The abundance of CO_2, CO, and organic species relative to water are prime metrics for physical conditions and radial mixing in the protosolar nebula. Abundance ratios may change as a comet evolves, so monitoring activity as comets progress through perihelion is important to quantifying evolutionary versus primordial signatures.

The NEOWISE debiased numbers suggest about 7 long-period comets 1 km or larger in size come within 1.5 AU of the Sun [19]. A comparison with present observations over the last 8 years suggests about 4.25 comets per year are detected that come within 1.5 AU on average, regardless of size. Probably more than half (about 60%) are detected, but a few remain undetected, assuming most of what we see have nuclei of >/= 1 km diameters. If we restrict these counts to inclinations of < 30 degrees, we get roughly 1.1 comets per year. If we restrict the set to comets that come within 1AU, our observations become closer to complete, with about 2.1 per year predicted, and 2 observed on average. We get about 0.35 per year that have inclination < 30, or one every 3 years or so, that would come with in 1 AU of the Sun. For the roughly co-planar shorter period comets (SPCs) (orbital period < 200 years), 7.6 SPCs that come within 1.5 AU of the Sun, and ~2.6 that come within 1AU, are observed per year. The inclination < 30 restriction makes little difference: ~7.3 are observed to come within 1.5 AU of the Sun on average per year, and 2.6 to come within 1 AU (no change).

Comet size distribution is important because it may affect visibility, potentially a factor in the current survey detections. There is also some debate as to whether the comet populations drop off with size below the ~1-4km size range too, but NEOWISE didn't see evidence of this. NEOWISE did see a couple comets down to ~500m in size, but these are small

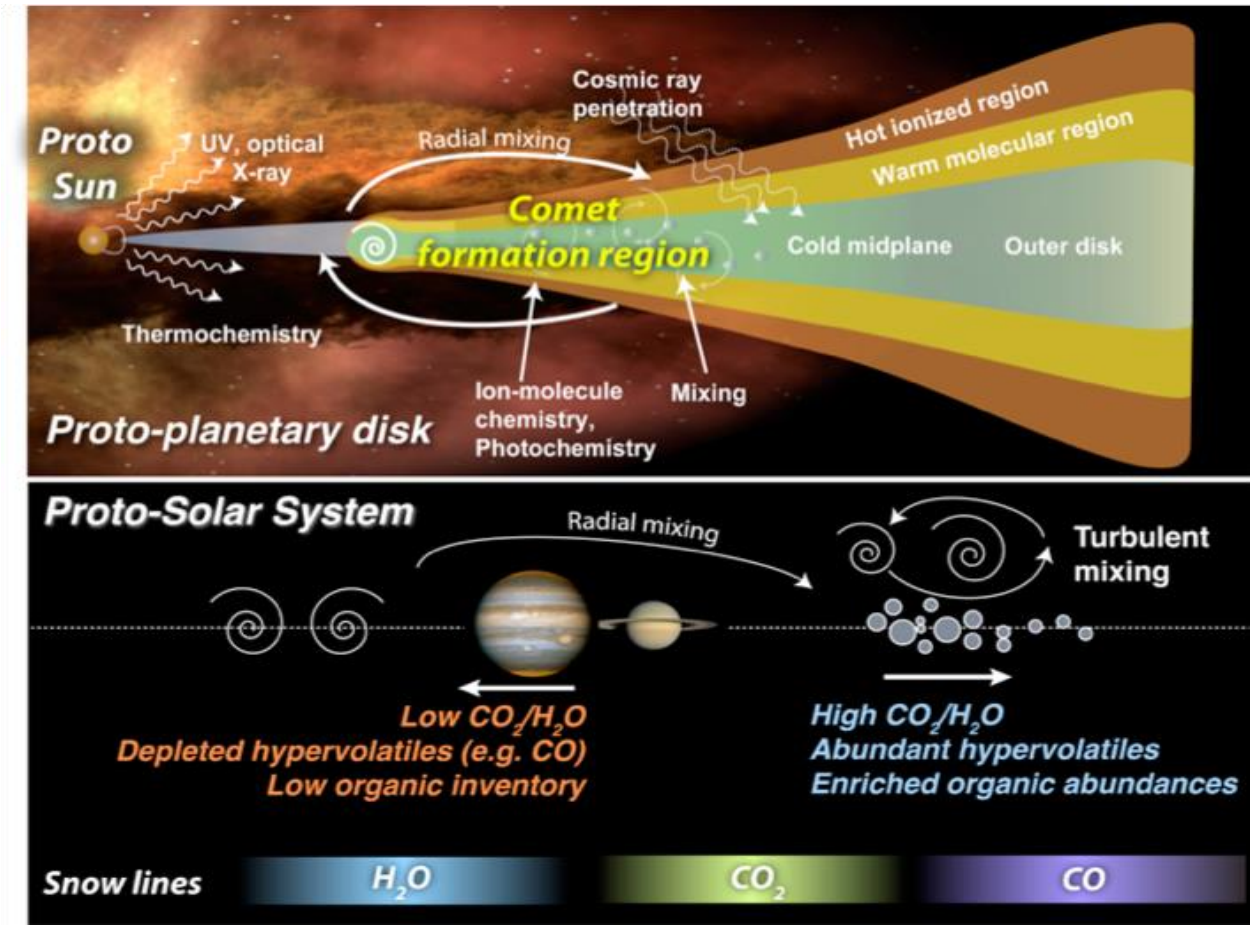

Figure 2: Comets as reflections of the solar system processes, formed during the proto-planetary disk phase and then subject to dynamic mixing. Do Oort cloud comets reflect the same diversity in composition and morphology seen in short period and Halley-type comets? See text for discussion. Drawing from Villanueva.

number statistics for a small size bin. For planning purposes, survey detection of a comet would be a necessary prerequisite for a visit. Should NEOCAM or LSST be commissioned and be capable of sampling comet flux down to sizes of ~500m, then NEOWISE suggests a linear boost in LPCs of about a factor of 2. For the SPC populations, finding objects down to 0.5km may produce a factor of 4 times as many SPCs as discussed in the previous paragraph.

2. OORT CLOUD COMETS

The Oort cloud, a vast, near-isotropic shell with heliocentric distance extending from ~1000 to ~200,000 AU, occupies the gravitational boundary of our SS. It stores OCC nuclei at cryogenic temperatures with minimal exposure to solar radiation, only subject to processing from cosmic rays. This enigmatic region is the primary source of long period and dynamically-new comets (LPCs), while the Kuiper Belt is the primary source of short period "ecliptic" comets [20,21], which include Encke-type comets and Jupiter-family comets such as 103P/Hartley 2, although an increasing body of evidence is suggesting that the reservoirs endured a lot more mixing and are less distinct than once thought. Ground- and space-based telescopes can observe OCCs, but only if one falls into the inner SS. Gravitational perturbations from passing stars cause OCCs to fall into the inner SS.

The NEOWISE sample of long-period comets (LPCs) is comprised of about 55% OCCs. The OCC is the noted reservoir of the LPC populations. The rate of OCCs that come within 1.5 AU of the Sun, in excess of 1km in diameter, is about 4 per year. For sizes down to 0.5km, about 8 per year achieve the same perihelion distances. Unlike periodic comets, OCCs

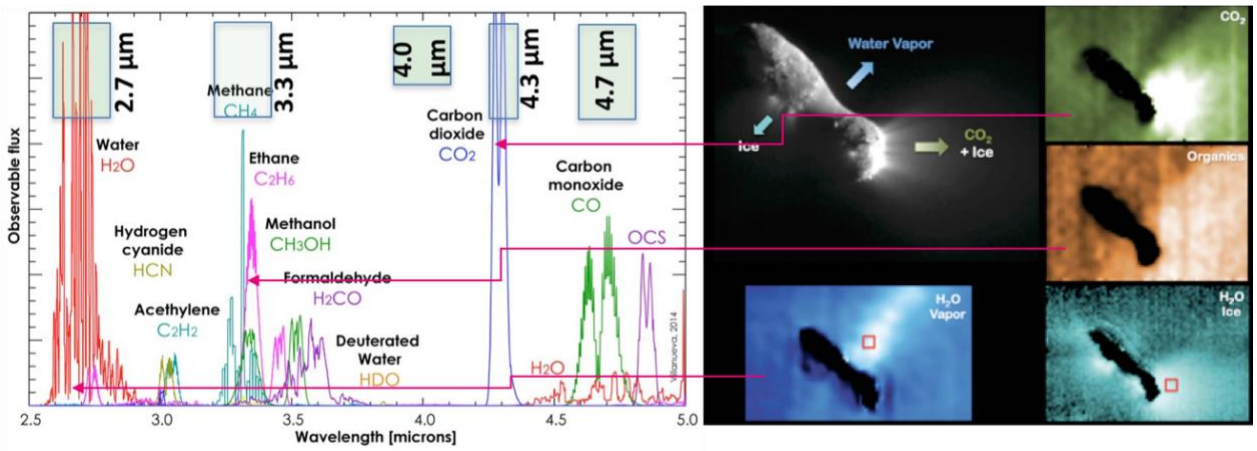

Figure 3. Cometary spectroscopy. Abundances and abundance ratios for water, carbon dioxide, carbon monoxide, and organics would establish the comet's formation conditions and region, as described in text. Synthetic spectra computed using the Planetary Spectrum Generator [22].

can have high orbital inclinations with respect to the ecliptic plane, which requires an encounter to be precisely at an ecliptic plane crossing node to minimize the off-ecliptic-plane distances.

3. MEASUREMENTS NEEDED

More measurements of cometary CO_2 are required to establish the formation region relative to the snow lines (distance from protostar where conditions lead to freezing) of volatiles H_2O, CO_2, and CO (**Figure 3**). As a result of the Akari and Deep Impact missions, CO_2 is now recognized as one of the most abundant volatiles in comets, yet we know relatively little about its diversity among comets. The abundance ratio of CO_2/H_2O varies widely among comets, by up to 25% for heliocentric distances $R_h < 2.4$ AU, and in some cases dominates the outgassing in comets for which $R_h > 3.5$ AU. A'Hearn et al. [18] suggest that high abundance and variability of CO_2 and CO could be explained by Long-Period-Comets (LPCs) and Jupiter-Family-Comets (JFCs) forming between the CO_2 and CO snow lines. Dynamical modelers and astrochemists investigating conditions in the protosolar nebula are integrating these findings and developing alternative formation scenarios. OCCs are expected to be highly active [23].

Severe telluric absorption prevents direct measurement of CO_2 concentrations in comets from the ground. Carbon dioxide concentrations thus have been measured in only the handful of comets observed or visited by spacecraft [24,25]. Indirect measurements of CO_2 have been inferred from the CO Cameron band and forbidden oxygen lines, yet these inferences are strongly model dependent [26,27,28,29]. The CO_2 retrievals from Akari are likely to be heavily affected by optical depth effects, as are other observations targeting the strong ν_3 fundamental band at 4.3 µm. Results from the Deep Impact spacecraft [30,17,15] need to be revised using realistic CO_2 and H_2O emission models including a detailed treatment of opacity to confirm the inferred outgassing morphologies and inner coma abundances.

4. PROVE CONCEPT

PrOVE would advance the science of primitive bodies by utilizing onboard propulsion or being delivered, potentially along with other identical payloads in a distributed network, to a libration or 'way' point orbit (Sun-Earth L1/L2, or lunar libration points) (**Figure 4**). There, PrOVE would remain, pending an opportunistic OCC discovery by ground- or space-based assets. With OCC orbital elements established by observatories, PrOVE would embark on a cruise phase to the ascending/descending node of the OCC orbit for a flyby encounter. At the encounter, PrOVE would acquire images of the nucleus and IR multispectral images to map coma volatiles with resolutions of up to 8 m (at 500 m).

Thus, the PrOVE mission would encompass an accessibility space that covers half the range of inclinations (0 to 90 degrees), out to 1.5 AU. The range of nucleus sizes for acquisition of target, facilitating early course-corrections, would extend down to ~500 meters in diameter. With these assumptions, approximately 4 OCCs would be accessible to PrOVE per year. Other limitations include the range of mean anomalies accessible to PrOVE, primarily in consideration of the

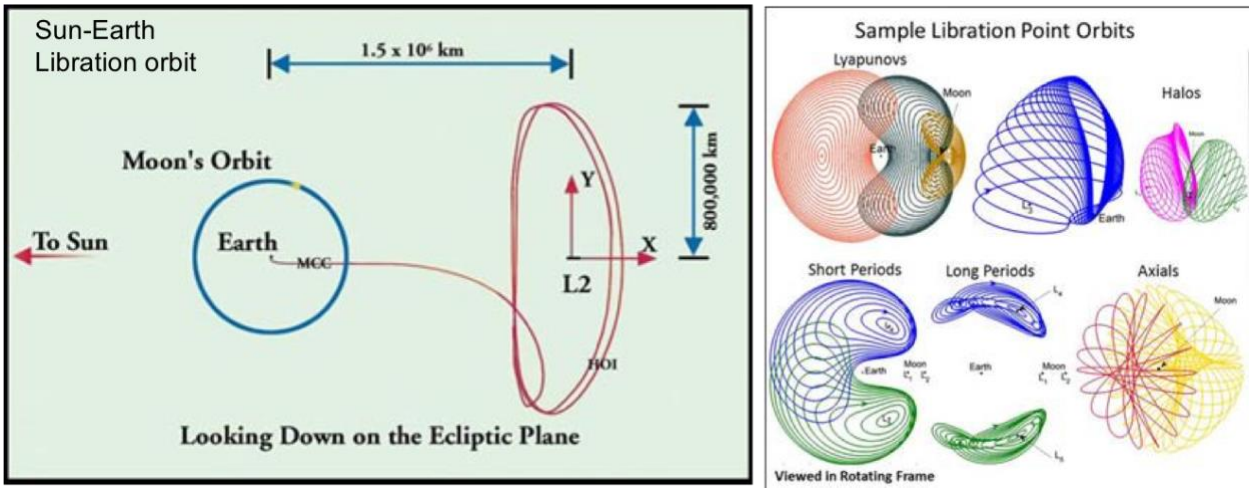

Figure 4. Waypoint storage, an essential aspect of the PrOVE mission concept, allowing a low energy, minimal resource way to wait for the next, typically unanticipated long period comet encounter opportunity. Waypoints are Sun-Earth libration points (left), and examples of halo or other stationkeeping (maintenance by propulsion) orbits are indicated on the right.

communication ranges of the spacecraft and specifically the Earth-Sun-PrOVE geometry. This could reduce the number of comets available to the spacecraft by a factor of 2. Still, the availability of 2 or more targets per year within the range of capabilities for study by a PrOVE encounter, would provide ample opportunity to select a target occupying lower-risk phase space for the multi-year mission. Historical statistics show ~3 OCCs are discovered annually.

Though its compact payload is certainly appropriate for a cubesat venue (<2 kg, <3U), 5W), PrOVE is currently configured as a 50 kg smallsat deployed near Earth, with a chemical propulsion system and conventional communication system. However, the components of a communication and transportation infrastructure in cislunar space are currently being tested or will be demonstrated over the next several years. The result could be not only transportation service to waypoints, but the availability of a high performance state of the art cubesat-scale propulsion system and onboard communication system. In either case, the demand for onboard performance would be considerably reduced, and a small standardized platform for PrOVE and other comet profilers could be an option [31].

The PrOVE science instruments were selected to provide high-quality, quantitative measurements of the physical state of the nucleus and chemical composition of the coma. These measurements would yield comprehensive maps of the primary cometary volatiles and thermal structure, and surface imaging at high-spatial resolution would reveal the morphology of a young surface with little exposure to solar insolation.

5. PROPOSED INSTRUMENTATION

The Rosetta mission obtained 3-m spatial resolution images of the periodic comet 67P. After smoothing this image to 9-m and 30-m, the PrOVE team determined <8-m spatial resolution requirement for a camera would enable PrOVE to acquire OCC images with sufficient resolution to resolve comparable surface relief. Based on this analysis, VisCAM optics were designed to provide a 3.3 arc-sec pixel field-of-view (IFOV) (8-m at 300 km) and >20 km x >15 km full FOV at 500 km. In order to provide measurements of the early solar system volatile inventory represented in the Oort Cloud, PrOVE would require an MWIR with spectral coverage spanning 2.5 to 5.0 microns. The MWIR spectrometer would also establish the continuum baseline for the thermal structure of the coma. An additional LWIR spectrometer would be required to provide heat flux measurements with <1K sensitivity.

The baseline PrOVE science instruments are two low-risk, high-TRL cameras: VisCAM, a visible camera and ComCAM, a multispectral IR imager. VisCAM is a Malin Space Science Systems (MSSS) CMOS camera based on the TAGCAMS

instrument on OSIRIS-REx. The camera core is TRL 9 and the high-resolution lens is TRL 6. ComCAM is an Institut National d'Optique (INO) multispectral camera with discrete focal plane integrated filters and a gold-black coated microbolometer array. ComCAM is currently TRL 4/5 and would need to be matured to TRL 6 by PDR.

6. VISCAM

VisCAM (**Figure 5**) is based on the proven MSSS ECAM-M50 camera head used in a variety of space missions (e.g., OSIRIS-REx TAGCAMS). An MSSS narrow FOV refractive telescope would be coupled to a MSSS ECAM-M50 camera core. The M50 uses a monochrome 2592 x 1944 pixel CMOS sensor with 2.2 µm pixels and an electronic rolling shutter. The camera head runs off regulated 5V power and a SpaceWire interface (10 MHz commanding, 100 MHz readout) to the spacecraft avionics. Subframe windowing can be commanded. Both the FPA and IFA boards are packaged closely in a single aluminum light weighted housing. The IFA functions include analog signal conditioning, FPA drives, low-level instrument control and data manipulation. The IFA provides all the clocks and biases required by the FPA to digitize the image sensor data to 12 bits. A preamplifier is located on the FPA to minimize the capacitive loading of the sensors analog output (s).

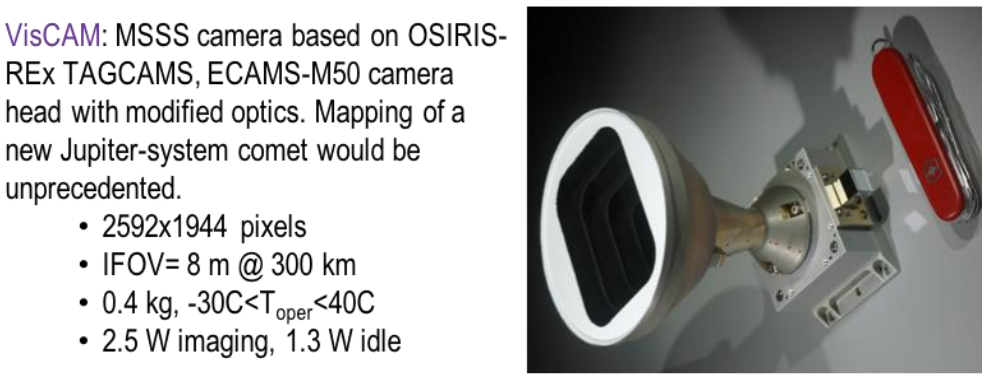

Figure 5. VisCAM Camera, a COTS low mass, volume, and power Malin Space Science Systems Camera with optics modified to allow 8 meter resolution at 300 km, as described in the text.

The PrOVE team in partnership with Malin Space Science Systems (MSSS) performed trade-off studies between different design solutions in order to satisfy all of PrOVE's VisCAM mission scientific objectives and requirements. This effort led us to the following design choices:

- a f#/4.3 lens telescope with excellent optical quality coupled with a framing detector, ensuring no mechanisms are implemented for yaw steering compensation;
- fine tuning of instrument parameters coupled with the mission design allows us to have an instrument designed to be fully compliant with both the high- and low-resolution imaging requirements of the mission and
- the instrument operations are flexible enough to optimize the acquisition parameters with respect to the many different observation requirements and conditions that PrOVE will face.

This instrument design would allow us to adjust the spatial resolution through binning, the field of view (FOV) through windowing, the signal levels and SNR through integration time and the instrument calibration parameters through in-flight calibration and data pre-processing. All the capabilities listed above would be guaranteed without imposing any requirement on the spacecraft (S/C) and without the use of any mechanisms. The current baseline instrument does not have a cover module; a risk assessment study would be done early on to evaluate any impact on instrument safety.

MSSS has designed, built, and flown over a dozen imaging systems for deep-space science missions (*e.g.*, 32,33,34). We would build VisCAM from the MSSS ECAM product line first released in 2013, a modular low-mass camera system intended to support in-flight engineering diagnostics, deployment/actuator monitoring, space situational awareness, and public outreach, as well as science applications. The first instance of an ECAM system for flight is the TAGCAMS for OSIRIS-REx. An image of the flight TAGCAMS is shown in **Figure 5**. Building on heritage from TAGCAMS [34], VisCAM would process images using a digital video recorder containing an eight gigabyte (GB) flash memory buffer and a space grade Xilinx Virtex-4 FPGA radiation tolerant [TID of 300 krad (Si) and LET of 100 MeVcm^2/mg] field programmable gate array (FPGA). The Xilinx FPGA can use any interface that operates with data transmission standard RS-422, low voltage differential signaling (LVDS), or discrete voltage levels with up to four signals in each direction. The

DVR would communicate with VisCAM using the SpaceWire (European Cooperation for Space Standardization 2008) protocol running at a maximum rate of 100 MHz. It would be powered from the host spacecraft using an unregulated 28 V power and distribute switched 5 V power to VisCAM.

7. COMCAM

ComCAM (**Figure 6**) is a filter radiometer designed to characterize the nucleus and coma by measuring temperatures and fluorescence emission from volatile species. The single focal plane camera that spans the MWIR and LWIR spectral regions implements a commercial microbolometer array [35] with heritage from the Aquarius mission, and a hyperspectral camera. Insolation near 1 AU results in molecular fluorescence at 2–5 µm (MWIR) and thermal emission from dust grains dominating >5µm (LWIR). The microbolometer, focal plane filter assembly, and telescope are TRL 5. Many mid-wave infrared (MWIR) focal plane arrays (FPA) technologies are capable of satisfying the spatial and spectral coverage requirements. However, the additional requirements for a low demand on PrOVE spacecraft resources and payload cost considerations make an uncooled microbolometer focal plane array (FPA) the optimal detector solution. MWIR information would be provided with <200 m resolution from 500 km with ~1% spatial co-registration between MWIR spectral bands, while maintaining 90° cross-track coverage and a ~45 km footprint at nadir (~100% clearance on each size of a 15 km comet nucleus). Use of the 288 pixels in the cross-track direction of a (384× 288) format FPA, would result in a 57 km swath with 200 m pixels. Its small size, low power, low mass, and minimal demands on the spacecraft make ComCAM a highly attractive solution to provide this information.

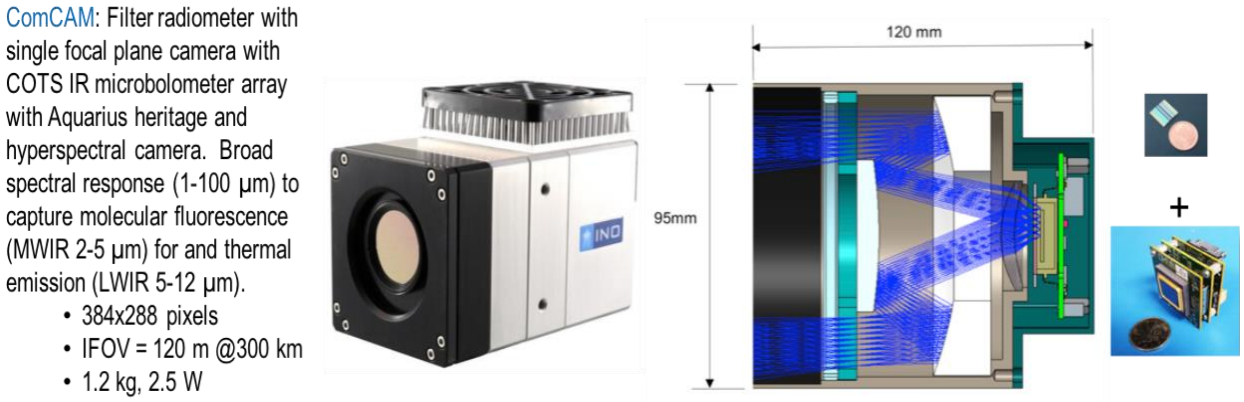

Figure 6. ComCAM filter radiometer with single focal plane camera and a commercial (INO) microbolometer array. The filter assembly has selected bands associated molecular species described above in the MWIR, and two channels for detecting thermal emission from dust grains in the LWIR.

ComCAM is configured as a pushbroom MWIR/LWIR imaging radiometer consisting of a commercial lens assembly, camera core, filter assembly, and proximity electronics. This complete sub-system would be manufactured by Institut National d'Optique (INO), Canada. The camera core is a VO_x microbolometer focal plane array (FPA) with an integrated complementary metal-oxide-semiconductor (CMOS) read out integrated circuit (ROIC). The strip band-pass filters are mounted directly onto the FPA. The FPA and the band-pass filters are at TRL>5 and leverage development efforts from other flight instruments (e.g., 36,37).

Five distinct spectral channels each with (48×384) pixels are defined by strip band-pass filters, manufactured on one substrate, and mounted directly onto the FPA. The five linear arrays are scanned across the target body as a pushbroom to build spectral images. ComCAM achieves high signal-to-noise ratio (SNR) in part by time delay integration (TDI) and pixel averaging. Imaging will be performed at ~100 km orbital altitude using an 80 mm aperture camera with fast optics (f#/1.05).

8. MISSION PROFILE

The mission profile is segmented into waypoint storage, cruise, followed, after a target is selected, by ingress, encounter, and egress periods during the single flyby of the OCC near its ascending node. We focus on the flyby here. The spacecraft

would be repositioned outside the encounter period so that the telescope can observe Earth and other Solar System objects (Moon, Jupiter, Venus, and Mars) for instrument calibration and bonus science.

Near cruise phase termination, comprehensive SOH and performance tests would be scheduled including bus check-out, Attitude and Control System (ACS) testing (pointing, slewing), science instrument check-out, instrument calibration. The encounter phase would start at ~1 Mkm from the comet. During ingress, the comet would be below and approaching PrOVE. At long range, each filter would be centered on the nucleus and sample a large area. At intermediate range, we would use the ACS to slowly rotate PrOVE and build a map of the coma. At closest encounter, we would use the spacecraft as a push-broom configuration and maintain position to image the nucleus. Attitude corrections would be employed as needed during the ingress and egress phases. The encounter phase would require careful pointing strategy to accommodate the ~11 km/s velocity of the comet relative to the spacecraft. Finally, the mission would convert to an egress observing modality, the mirror image of the ingress sequence. As the spacecraft approached the comet, the spatial resolution would get finer. Near closest encounter, ComCAM pixel resolution would be ~0.3 km and span a width of ~40 km. VisCAM resolution would be about ~8 m. The encounter data would be recorded in spacecraft storage for post-encounter downlink. This strategy provides for our baseline science with global coverage maps by filter channel.

9. ACKNOWLEDGMENT

This material based on work supported by NASA under 16-PSDS316-0009 issued through the Planetary Science Deep Space SmallSat Studies Program. Portion of work at Jet Propulsion Laboratory, California Institute of Technology under contract with NASA. The information in this document is pre-decisional and is for information and discussion purposes only.

REFERENCES

[1] Mumma, M. and S. Charnley (2011) The chemical composition of comets - emerging taxonomies and natal heritage, Ann Rev of Astronomy and Astrophysics, 49, 471-524.
[2] Gomes, R., H. Levison, K. Tsiganis, A. Morbidelli (2005) Chaotic capture of Jupiter's Trojan asteroids in the early Solar System, Nature 435, 466-469.
[3] Morbidelli, A., H. Levison (2008) Late evolution of planetary systems, Physica Scripta T130 014028 (6pp)
[4] Crovisier J. (2006) Recent results and future prospects for the spectroscopy of comets, Molecular Physics, 104, 16-17, 2737-2751.
[5] Morbidelli, A., H. Levison, K. Tsiganis, R. Gomes (2005) Chaotic capture of Jupiter's Trojan asteroids in the early solar system, Nature, 435, 462-465.
[6] Dones, L., R. Brasser, N. Kaib, H. Rickman (2015) Origin and evolution of Cometary Reservoirs, Space Science Reviews, 197, 1-4, 191-269.
[7] Dello Russo, N., R. Vervack, H. Weaver, H. Kawakita, H. Kobayashi, N. Biver, D. Bockelee-Morvan, J. Crovisier (2009) The parent volatile composition of 6P/d'Arrest and a chemical comparison of Jupiter-family comets measured at infrared wavelengths, Astrophysical Journal, 703, 1, 187-197.
[8] Disanti, M. and M. Mumma (2008) Reservoirs for comets: Compositional differences based on infrared observations, Space Science Reviews, 138, 1-4, 127-145.
[9] Bockelée-Morvan, D, N. Biver, O. Colom, J. Crovisier, F. Henry, A. Lecacheux, J. Davies, W. Dent, H Weaver (2004) The outgassing and composition of Comet 19P/Borrelly from radio observations, Icarus, 167, 1, 113-128.
[10] A'Hearn, M., R. Millis, D. Schleicher, D. Osip, P. Birch (1995) The ensemble properties of comets: results from narrowband photometry of 85 comets, 1976-1992, Icarus, 118, 2, 223-270.
[11] Fink, U. and M. Hicks (1996) A survey of 39 comets using CCD spectroscopy, Astrophysical Journal, 459, 2, 729-743.
[12] Cochran, A., H. Levison, P. Tamblyn, S. Stern, M. Duncan (1998) The calibration of the Hubble Space Telescope Kuiper belt object search: setting the record straight, Astrophysical Journal, 503, 1, L89-L93.
[13] [Levison, H., M. Duncan, R. Brasser, (2010) Capture of the Sun's Ooort cloud from stars in its birth cluster. Science, 329, 5988, 187-190.

[14] Ootsubo, T., H. Kawakita, S. Hamada, (2012) Akari near-infrared spectroscopic survey for CO2 in 18 comets, Astrophysical Journal, 752, 1, 15.
[15] Feaga, L., M. A'Hearn, J. Sunshine, O. Groussin, T. Farnham (2007) Asymmetries in the distribution of H(2)O and CO(2) in the inner coma of Comet 9P/Tempel 1 as observed by Deep Impact, Icarus, 190, 2, 345-356.
[16] Feaga, L., M. A'Hearn, T. Farnham, D. Bodewits, J. Sunshine, A. Gersch, S. Protopapa, B. Yang, M. Drahus, D. Schleicher (2014) Uncorrelated volatile behavior during the 2011 apparition of Comet C/2009 P1 Garradd, Astronomical Journal, 147, 1, 24.
[17] A'Hearn, M., M. Belton, W. Delamere, W, L. Feaga, D. Hampton, J. Kissel, K. Klaasen, L. McFadden, K. Meech, H.J. Melosh (2011) EPOXI at Comet Hartley 2, Science, 332, 6036, 1396-1400.
[18] A'Hearn, M., L. Feaga, H. Keller, H. Kawakita, D. Hampton, J. Kissel, K. Klaasen, L. McFadden, K. Meech, P. Schultz (2012) Cometary volatiles and the origin of comets, Astrophysical Journal, 29, 758, 1, 0004-637X.
[19] Bauer, J., T. Grav, Y. Fernandez, A. Mainzer, E. Kramer, J. Masiero, T. Spahr, C. Nugent, R. Stevenson, K. Meech (2017) Debiasing the NEOWISE cryogenic mission comet populations, Astronomical Journal, 154, 2, 53 (9pp).
[20] Bernstein, G., D. Trilling, R. Allen, M. Brown, M Holman, R. Malhotra (2004) The size distribution of trans-Neptunian bodies, Astronomical Journal, 128, 3, 1364-1390.
[21] Gladman, B. (2005) The Kuiper belt and the solar system's comet disk, Science, 307, 5706, 71-75.
[22] Villanueva, G. , M. Smith, S. Protopapa, S. Faggi, A. Mandell (2018) Planetary spectrum generator: An accurate online radiative transfer suite for atmospheres, comets, small bodies, and exoplanets, J. Quantitative Spectroscopy and Radiative Transfer, 217, 86-104.
[23] [Farnham, T. and D. Schleicher (1998) Narrowband photometric results for comet 46P/Wirtanen, Astronomy & Astrophysics, 335, 2, L50-L55.
[24] [Combes, M. V. Moroz, J. Crovisier, T. Encrenaz, J. Bibring, A. Grigoriev, N. Sanko, N. Coron, J. Crifo, R. Gispert (1988) The 2.5-12 Mu-M spectrum of comet Halley from the IKS-Vega Experiment, Icarus, 76, 3, 404-436.
[25] Crovisier, J., T. Brooke, M. Hanner, H. Keller, P. Lamy, B. Altieri, D. Bockelee-Morvan, L. Jorda, K. Leech, E. Lellouch (1996) The infrared spectrum of comet C/1995 O1 (Hale-Bopp) at 4.6 AU form the sun, Astronomy & Astrophysics, 315, 2, L385-L388.
[26] [Weaver, H., P. Feldman, J. McPhate, (1994) Detection of CO Cameron band emission in Comet P/Hartley-2 (1991 XV) with the Hubble Space Telescope, Astrophysical Journal, 422, 1, 374-380.
[27] Feldman, P. M. Festou, G. Tozzi, (1997) The CO2/CP abundance ratio in 1P/Halley and several other comets observed by IUE and HST, Astrophysical Journal, 475, 2, 829&Part:1.
[28] McKay, A., N. Chanover, J. Morgenthaler, A. Cochran, W. Harris, N. Dello Russo (2013) Observations of the forbidden oxygen lines in DIXI target Comet 103P/Hartley, Icarus, 222, 2, SI, 684-690.
[29] McKay, A., A. Cochran, M. DiSanti, G. Villanueva, N. Dello Russo, R. Vervack, J. Morgenthaler, W. Harris, N. Chanover (2015) Evolution of H2O, CO, CO2 production in Comet C/2009 P1 Garradd during the 2011-2012 apparition, Icarus, 50, 504-515.
[30] [A'Hearn, M., M. Belton, W. Delamere, J. Kissel, K. Klaasen, L. McFadden, K. Meech, H.J. Melosh, P. Schultz, J. Sunshine (2005) Deep Impact: Excavating comet Tempel 1, Science, 310 5746, 258-264.
[31] Clark, P.E., R. MacDowall, W. Farrell, C. Brambora, A. Lunsford, T. Hurford, D. Folta, B. Malphrus, M. Grubb, S. Wilzcewski, E. Bujold (2018) Nature of and lessons learned from Lunar Ice Cube and the first deep space cubesat 'cluster', Proc SPIE this issue.
[32] Christensen, P., B. Jakosky, H. Kieffer, M. Malin, H. McSween, K. Nealson, G. Mehall, S. Silverman, S. Ferry, M. Caplinger (2004) The THermal Emission Imaging System (THEMIS) for Mars 2001 Odyssey Mission, Space Science Reviews, 110, 1-2, 85-130.
[33] Malin, M., J. Bell, B. Cantor, M. Caplinger, W. Calvin, R. Clancy, K. Edgett, L. Edwards, R. Haberle, P. James (2007) Context camera investigation on board the Mars Reconnaissance Orbiter, JGR-Planets, 112, E5, E05504.
[34] Robinson, M., S. Brylow, M. Tschimmel, D. Humm, S. Lawrence, P. Thomas, B. Denevi, E. Bowman-Cisneros, J. Zerr, M. Ravine (2010) Lunar Reconnaissance Orbiter Camera (LROC) instrument overview, Space Science Reviews, 150, 14, 81-124.
[35] Bos, B., M. Ravine, M. Caplinger, (2018) Touch and Go Camera System (TAGCAMS) for the OSIRIS-REx asteroid sample return mission, Space Science Reviews, 214, 1, UNSP37.
[36] Pope, A., R. Chary, D. Alexander, L. Armus, M. Dickinson, D. Elbaz, D. Frayer, D. Scott, H. Teplitz (2008) Mid-Infrared spectral diagnosis of submillimeter galaxies, Astrophysical Journal, 675, 2, 1171-1193.
[37] Manizade, K., J. Spinhirne, R. Lancaster (2006) Stereo cloud heights from multispectral IR imagery via region-of-interest segmentation, IEEE Trans Geoscience and Remote Sensing, 44, 9, 2481-2491.